Large-scale shell model study of the newly found isomer in ^{136}La

E. Teruya,[1,*] N. Yoshinaga,[1,†] K. Higashiyama,[2,‡] H. Nishibata,[3] A. Odahara,[3] and T. Shimoda[3]
[1]*Department of Physics, Saitama University, Saitama City 338-8570, Japan*
[2]*Department of Physics, Chiba Institute of Technology, Narashino, Chiba 275-0023, Japan*
[3]*Department of Physics, Osaka University, Osaka 560-0043, Japan*
(Received 13 May 2016; published 21 July 2016)

The doubly-odd nucleus ^{136}La is theoretically studied in terms of a large-scale shell model. The energy spectrum and transition rates are calculated and compared with the most updated experimental data. The isomerism is investigated for the first 14^+ state, which was found to be an isomer in the previous study [Phys. Rev. C **91**, 054305 (2015)]. It is found that the 14^+ state becomes an isomer due to a band crossing of two bands with completely different configurations. The yrast band with the $(\nu h_{11/2}^{-1} \otimes \pi h_{11/2})$ configuration is investigated, revealing a staggering nature in $M1$ transition rates.

DOI: 10.1103/PhysRevC.94.014317

I. INTRODUCTION

Studies of a doubly-odd nucleus give us a lot of information not only on the doubly-odd nucleus itself, but also on the neighboring even-even and odd-mass nuclei. As a naive description, the doubly-odd nucleus can be simply viewed in terms of a one-neutron and one-proton configuration coupled with the corresponding even-even core. In the vicinity of mass 130, where the nucleus has a few neutron holes from the magic number 82 and a few proton particles from the magic number 50, the $0h_{11/2}$ intruder orbital plays a particularly important role among the five orbitals ($0g_{7/2}$, $1d_{5/2}$, $2s_{1/2}$, $0h_{11/2}$, and $1d_{3/2}$) since it has different parity from others and also it has the largest spin among all of them. Thus one characteristic feature of the doubly-odd nuclei in this region is seen in the existence of bands which have the $(\nu h_{11/2}^{-1} \otimes \pi h_{11/2})$ configuration.

In ^{136}La, several experimental observations were carried out and a typical $(\nu h_{11/2}^{-1} \otimes \pi h_{11/2})$ band has been observed in some literature [1–4]. However, the proposed level schemes are not consistent with each other. In the most recent paper [4], a detailed experimental investigation was performed and the level scheme was newly constructed. A new isomer of spin-parity 14^+ with a half-life of 187(27) ns was found at an excitation energy of around 2.3 MeV. This isomer is peculiar since no such long-lived isomer has been observed yet at high spin in odd-odd nuclei in the $A = 130$–140 mass region. In the same paper, energy levels were theoretically investigated using the pair-truncated shell model (PTSM). However, the isomerism of the 14^+ state has not been unveiled yet.

Nuclei around mass 130 were analyzed using the PTSM [5–8] and the shell model [9,10]. The structure of the $(\nu h_{11/2}^{-1} \otimes \pi h_{11/2})$ bands were also analyzed using a simple model termed the quadrupole coupling model [11–14]. Recently, systematic studies were carried out for even-even, odd mass, and doubly-odd nuclei around mass 130 using the shell model [10]. In that work energy levels and electromagnetic properties of 46 nuclei were calculated adopting only one set of the two-body interaction strengths, and detailed analyses for some specific nuclei were carried out. Several isomers were analyzed and were classified as spin-gap isomers or seniority isomers by their reasons for existence.

In this paper, a large-scale shell model calculation is performed for ^{136}La. One aim of this study is to elucidate the isomerism of the first 14^+ state through the analysis of the neighboring states around the 14^+ state. Another purpose is to analyze the structure of the yrast band with the $(\nu h_{11/2}^{-1} \otimes \pi h_{11/2})$ configuration.

This paper is organized as follows. The general framework of the present shell-model study is given in Sec. II. The calculated results are presented and compared with the experimental results in Sec. III. The isomerism of the 14^+ state is discussed and the analysis of the $(\nu h_{11/2}^{-1} \otimes \pi h_{11/2})$ band is given. Finally this work is summarized in Sec. IV.

II. THEORETICAL FRAMEWORK

A large-scale shell model calculation is performed for ^{136}La. This nucleus is a system with three neutron holes and seven proton particles assuming the ^{132}Sn nucleus as a doubly magic core. The framework of the calculation is the same as that used for the systematic shell-model calculation for nuclei around mass 130 [10]. For a description of ^{136}La, all five single-particle orbitals between the magic numbers 50 and 82 ($0g_{7/2}$, $1d_{5/2}$, $2s_{1/2}$, $0h_{11/2}$, and $1d_{3/2}$) are taken into account for both neutrons and protons. The single-particle energies employed in this study are the same as those adopted in Ref. [10].

As for the phenomenological interaction, the two-body interaction consisting of multipole-pairing interactions in addition to the pairing plus quadrupole-quadrupole interaction is employed. In this study, two kinds of parameter sets for the strengths of two-body interactions are used. One set (Set A) adopts strengths which are completely the same as those in Ref. [10]. Another set (Set B) adopts those strengths which are almost the same as those in Ref. [10], but only two strengths are modified a little for a better description of the energy spectra for ^{136}La in the present approach. Table I shows the set of

*teruya@nuclei.th.phy.saitama-u.ac.jp
†yoshinaga@phy.saitama-u.ac.jp
‡koji.higashiyama@it-chiba.ac.jp

TABLE I. Modified strengths of adopted two-body interactions between neutrons (ν-ν), protons (π-π), and neutrons and protons (ν-π). G_0 and G_2 indicate the strengths of the monopole pairing (MP) and quadrupole-pairing (QP) interactions between like nucleons, respectively. G_L ($L = 4,6,8,10$) denote the strengths for higher multipole-pairing (HMP) interactions between like nucleons. The κ_2's indicate the strengths of the quadrupole-quadrupole (QQ) interactions between like and alike nucleons. The strengths of the MP and HMP interactions are given in units of MeV. The strengths of the QP and QQ interactions are given in units of MeV/b^4 using the oscillator parameter $b = \sqrt{\hbar/(M\omega)}$. Blanks mean that no strengths are employed.

	G_0	G_2	G_4	G_6	G_8	G_{10}	κ_2
ν-ν	0.170	0.018	1.00	−2.00	−6.15	−14.0	0.010
π-π	0.165	0.007	0.20	0.10			0.055
ν-π							−0.080

strengths (Set B) of the modified interaction for ^{136}La. The strength of the quadrupole-quadrupole interaction between neutrons and protons, $\kappa_{2\nu\pi}$, is changed from $\kappa_{2\nu\pi} = -0.100$ used in Ref. [10] to $\kappa_{2\nu\pi} = -0.080$ and the strength of the hexadecapole-pairing interaction between neutrons $G_{4\nu}$, is changed from $G_{4\nu} = -0.50$ used in Ref. [10] to $G_{4\nu} = +1.00$.

In this framework the shell-model states are classified as four classes: $(+,+)$, $(+,-)$, $(-,+)$, and $(-,-)$ according to the parity in the neutron space or in the proton space. Parity of any states belonging to the $(+,+)$ class is positive for the neutron part and also positive for the proton part, which is hereafter denoted as the state with the $(+,+)$ configuration. Parity of any states in the $(-,-)$ class is negative for the neutron part and also negative for the proton part, which is denoted as the state with the $(-,-)$ configuration. In this shell-model study, any kind of two-body interaction which admixes a neutron in a certain parity orbital and a proton in the opposite parity orbital is not introduced. Therefore states with the $(+,+)$ configuration and those with the $(-,-)$ configuration are not mixed with each other.

For this nucleus, the shell-model dimension for diagonalization is too large to perform a full calculation without any truncation. Thus it is necessary to truncate the shell-model dimension. In this study, the same truncation scheme described in Sec. II B of Ref. [10] is adopted. All calculations are performed with the truncation of $L_c = 500$. Here the definition of L_c is the same as given in Eq. (22) in Ref. [10]. The convergence of energy levels up to excitation energy of 3 MeV has been confirmed by increasing L_c. The details of the framework and the Hamiltonian for diagonalization are given in Ref. [10].

III. NUMERICAL RESULTS AND DISCUSSION

The calculated low-lying energy levels for both positive- and negative-parity states are shown in Fig. 1 in comparison with the experimental data [4,15]. In this figure, the experimental (7_1^-) state at $0.00 + x$ MeV is shown under assumption of $x = 0.03$. For the theoretical results, two lowest positive-parity states with the same spin are shown among many calculated states.

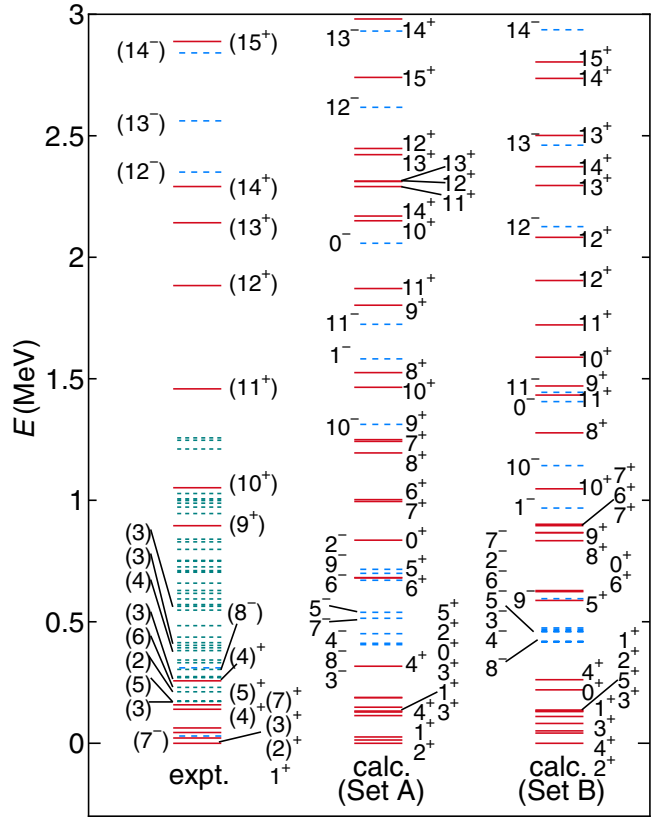

FIG. 1. Calculated energy spectra up to 3.0 MeV for ^{136}La (calc.) in comparison with the experimental data (expt.) [4,15]. For theoretical results, the calculation with the strength set used in Ref. [10] [calc. (set A)] and the calculation with the modified strength set [calc. (Set B)] are shown. States with positive (negative) parity are shown with solid (dashed) lines. Experimentally parity-unassigned states are shown with dotted lines.

One-to-one correspondence is seen in between the experimental data and the calculated results. Using the parameter set of the previous study (Set A), positive-parity states above the 9_1^+ state are calculated about 0.5 MeV higher than the experimental ones. In contrast the theoretical calculation using the parameter set of modified strengths (Set B) well reproduces most of the experimental data. The calculated 7_1^- state is predicted higher than the experimental one for both calculated results (Sets A and B). It is necessary to introduce other kinds of interactions to reproduce the energy of the (7_1^-) state, such as an octupole interaction between neutrons and protons.

Figure 2 shows the calculated energy levels only for positive-parity states in comparison with the experimental data [4,15]. The calculated 7_1^+ state is much higher than the experimental (7_1^+) state at 0.030 MeV above the (7_1^-) state [4] in both cases (Sets A and B). Note that this experimental (7_1^+) assignment was performed [4] by the group in which most of the authors of the present paper are involved. This assignment is assumed by taking into account the (9^+) assignment for the 0.865-MeV state and the reported $E2$ nature [1] of the deexciting transition to the 0.030-MeV state.

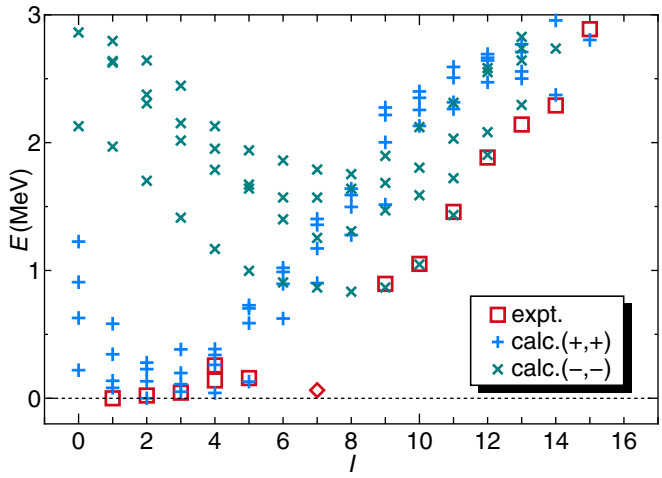

FIG. 2. Calculated energy levels for positive-parity states using the modified interaction (Set B) in comparison with the experimental data [4,15]. The legend "calc.(+,+)" represents theoretical results for the (+,+) configuration and "calc.(−,−)" represents theoretical results for the (−,−) configuration. Calculated states are shown up to four levels with the same configuration for each spin. Spin and parity of the state at 0.03 MeV is assigned as the (7^+) state in experiment (shown with the diamond). However, there are other possibilities for this assignment (see text).

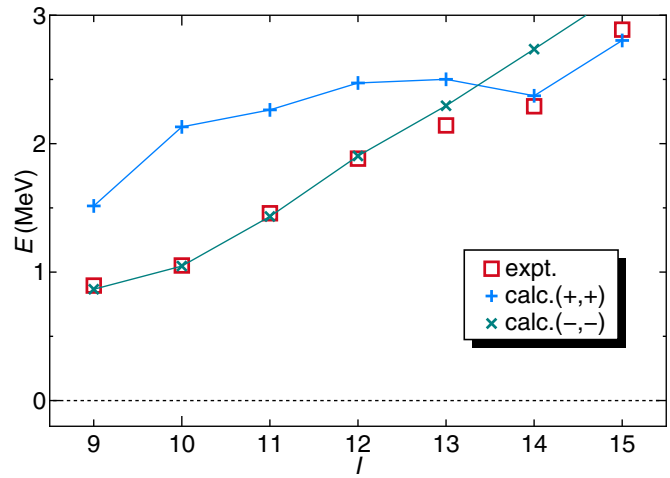

FIG. 3. Calculated positive-parity yrast states with the (+,+) and (−,−) configurations with $I \geqslant 9$ in comparison with the experimental data.

Although the (9^+) assignment seems rather reasonable in the La isotope systematics of the $(\nu h_{11/2}^{-1} \otimes \pi h_{11/2})$ bands, no convincing DCO (directional correlation from oriented states) ratio data, which provide information on the multipolarity of the transition [1–3], are available for the $E2$ assignment. Therefore, another assignment, such as a negative-parity one, is also possible for the 0.030-MeV state. The fact that the present shell-model calculation predicts no positive-parity states with spin $I \geqslant 6$ in the very-low-excitation energy region supports the negative-parity assignment for this state. In the following, all the theoretical results are shown with the modified strength set (Set B).

Next, the isomerism of the 14_1^+ state is analyzed. In Fig. 2 the legend "calc.(−,−)" represents states with the (−,−) configuration. Namely, these states have the $(\nu h_{11/2}^{-1} \otimes \pi h_{11/2})$ configuration, since only the $0h_{11/2}$ orbital is a negative-parity orbital in this region. The legend "calc.(+,+)" represents states with the (+,+) configuration.

To understand the structural change of high spin yrast states more clearly, Fig. 3 shows the calculated yrast states with the (+,+) and (−,−) configurations with $I \geqslant 9$ in comparison with the experimental data. As seen in the figure, the 9_1^+, 10_1^+, 11_1^+, 12_1^+, and 13_1^+ states are members of a group with the (−,−) configuration. In contrast, the 14_1^+ and 15_1^+ states are members of a group with the (+,+) configuration. Because of this structural change between the 13_1^+ and 14_1^+ states, electromagnetic transitions from the 14_1^+ state to the 13_1^+ state are strictly forbidden theoretically. Namely, there occurs a band crossing from a band with the (−,−) configuration to a band with the (+,+) configuration.

Another important fact is that the 13^+ and 12^+ states with the (+,+) configuration are located higher than the 14_1^+ state. Thus the 14_1^+ state does not decay to the 13^+ and 12^+ states with the (+,+) configuration. Because of these kinds of reasons, the 14_1^+ state becomes the isomer.

Figure 4 shows the experimental and theoretical kinematic moment of inertia $\mathcal{J}(I)$, which is defined as

$$\mathcal{J}(I) = \frac{2I-1}{E(I)-E(I-2)}. \quad (1)$$

A good agreement between the experimental data and the shell-model results is seen. The theoretical moment of inertia for the 15_1^+ state does not agree with the experimental one, which is largely due to the fact that energy of the theoretical 13_1^+ state is calculated 0.15 MeV higher than the experimental one. As mentioned before, any kind of two-body interaction which admixes states with the (+,+) configuration and those with the (−,−) configuration has not been introduced in the present work. If such kinds of interactions are introduced, the 13_1^+ state

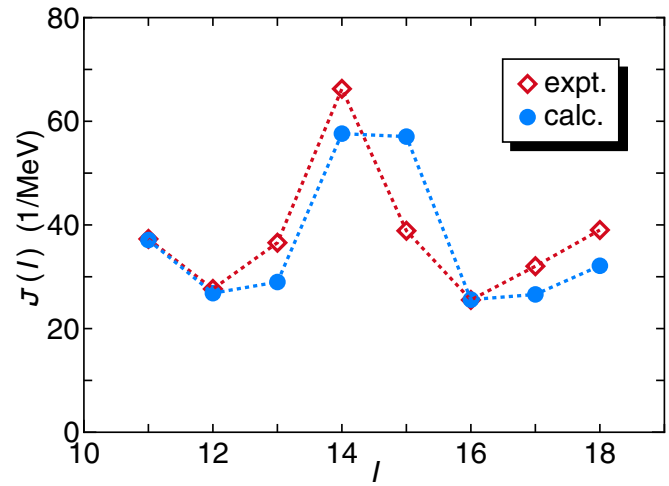

FIG. 4. Comparison of the kinematic moment of inertia $\mathcal{J}(I)$ between the experimental results and the theoretical ones.

TABLE II. Calculated occupation number in each orbital for the 14_1^+ state.

	Orbital				
	$s_{1/2}$	$d_{3/2}$	$d_{5/2}$	$g_{7/2}$	$h_{11/2}$
Neutron	0.009	0.959	0.015	0.017	2.000
Proton	0.171	0.341	1.993	4.114	0.381

would get lower in energy, whereas the 13_2^+ state would get higher in energy by avoiding each other due to the repulsive interaction between them. That might explain the discrepancy between experiment and theory for the energy gap between the 13_1^+ state and the 13_2^+ state.

Table II shows the calculated occupation number in each orbital, $v_j^2(i)$, for the 14_1^+ state. The occupation number in the single-particle orbital j for the ith eigenstate with spin I_i ($|\Phi(I_i;i)\rangle$) is defined as

$$v_j^2(i) = \langle\Phi(I_i;i)|\hat{n}_j|\Phi(I_i;i)\rangle, \tag{2}$$

where the particle number operator $\hat{n}_j$ in the j orbital is given as

$$\hat{n}_j = \sum_m c_{jm}^\dagger c_{jm}. \tag{3}$$

Here $c_{jm}^\dagger$ and c_{jm} are the nucleon creation and annihilation operators in the orbital j with its projection m. As seen in Table II, our calculation shows that, for the neutron part of the 14_1^+ state, two valence neutrons of the three occupy the $h_{11/2}$ orbital and the odd neutron occupies the $d_{3/2}$ orbital. For the proton part, the occupation number in the $h_{11/2}$ orbital is 0.381. This indicates that the 14_1^+ state is a mixture of the following two states: (i) no protons occupying the $h_{11/2}$ orbital and (ii) two protons occupying the $h_{11/2}$ orbital, since the 14_1^+ state belongs to the $(+,+)$ configuration. A detailed calculation shows that 84% of the 14_1^+ state is constructed by the state (i).

The lowest 14^+ state with the $(\nu h_{11/2}^{-1} \otimes \pi h_{11/2})$ configuration, which is the second 14^+ state, is calculated 0.36 MeV higher than the 14_1^+ state with the $(+,+)$ configuration. Table III shows the calculated occupation number in each orbital for the 14_2^+ state with the $(\nu h_{11/2}^{-1} \otimes \pi h_{11/2})$ configuration. The occupation number (1.869) of the $\nu h_{11/2}$ orbital indicates that the 14_2^+ state is a mixture of the $(\nu h_{11/2}^{-1} \otimes \pi h_{11/2})$ and $(\nu h_{11/2}^{-3} \otimes \pi h_{11/2})$ configurations.

Figure 5 shows the calculated $B(E2)$, $B(M1)$, and $B(M1)/B(E2)$ values among the yrast states and those among the states with the $(\nu h_{11/2}^{-1} \otimes \pi h_{11/2})$ configuration. Here the

TABLE III. Calculated occupation number in each orbital for the 14_2^+ state [the lowest 14^+ state with the $(\nu h_{11/2}^{-1} \otimes \pi h_{11/2})$ configuration].

	Orbital				
	$s_{1/2}$	$d_{3/2}$	$d_{5/2}$	$g_{7/2}$	$h_{11/2}$
Neutron	0.194	0.751	0.114	0.072	1.869
Proton	0.175	0.332	1.879	3.501	1.113

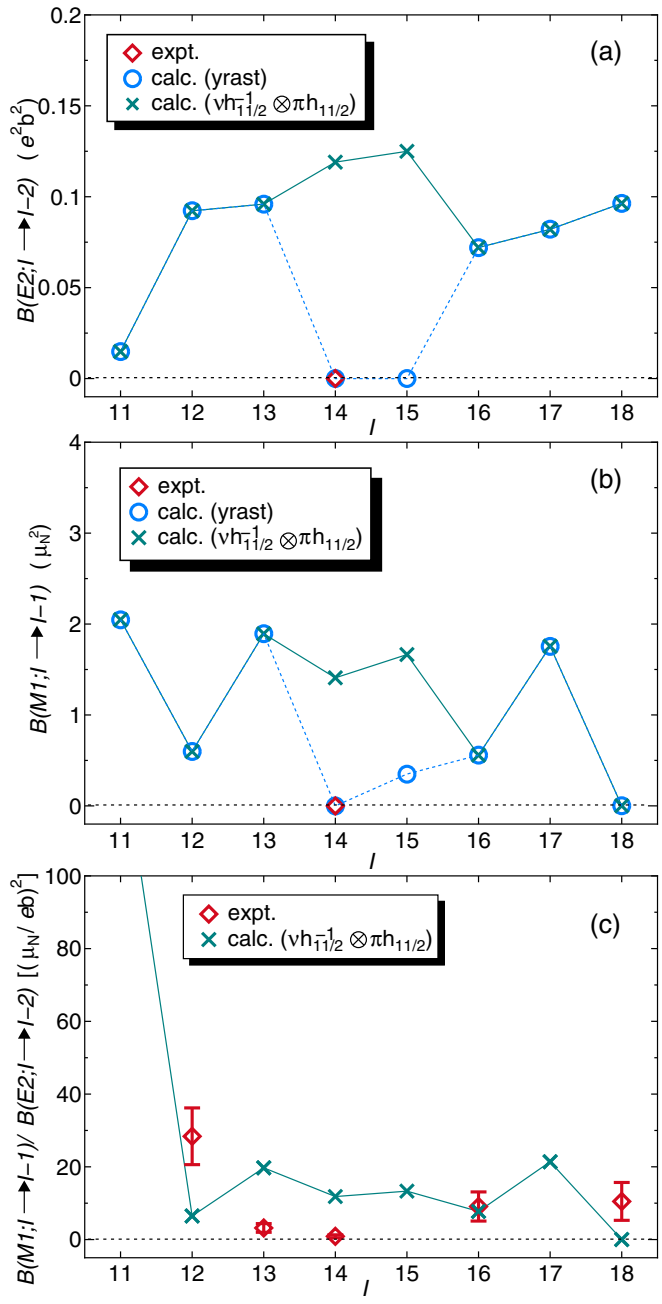

FIG. 5. (a) Calculated $B(E2)$, (b) $B(M1)$, and (c) $B(M1)/B(E2)$ values among the yrast states and the $(\nu h_{11/2}^{-1} \otimes \pi h_{11/2})$ configurations in comparison with the experimental data [4]. Yrast states are connected by dotted lines and the states with the $(\nu h_{11/2}^{-1} \otimes \pi h_{11/2})$ configuration are connected by solid lines.

effective charges and gyromagnetic ratios are exactly the same as those adopted in Ref. [10]. The experimental values, $B(M1; 14_1^+ \to 13_1^+) = 1.9 \times 10^{-3}\ \mu_N^2$ and $B(E2; 14_1^+ \to 12_1^+) = 1.9 \times 10^{-5}\ e^2\text{b}^2$ [4], are also shown in the figure. The theoretical $B(E2; 14_1^+ \to 12_1^+)$, $B(E2; 15_1^+ \to 13_1^+)$, and $B(M1; 14_1^+ \to 13_1^+)$ values all exactly vanish, although the theoretical $B(E2; 14_1^+ \to 12_1^+)$ and $B(M1; 14_1^+ \to 13_1^+)$ values seemingly agree with the experimental data in Fig. 5. In this shell-model framework, states with the $(+,+)$ configuration

and those with the $(-,-)$ configuration are not mixed. Thus $M1$ and $E2$ transition rates between states with the $(+,+)$ configuration (the 14_1^+ and 15_1^+ states) and states with the $(-,-)$ configuration (the 12_1^+ and 13_1^+ states) vanish.

In order to give the finite $B(E2;14_1^+ \to 12_1^+)$ and $B(M1;14_1^+ \to 13_1^+)$ values theoretically, it is necessary to introduce two-body interactions, such as an octupole interaction, which admix states with the $(+,+)$ configuration and states with the $(-,-)$ configuration. Such kinds of interactions between neutrons and protons are requiredto get finite $E2$ or $M1$ transition rates since originally the 12_1^+ and 13_1^+ states consist only of the $(+,+)$ configuration and the 14_1^+ state consists only of the $(-,-)$ configuration.

Suppose that the original 14_1^+ and 13_1^+ states are admixed as follows:

$$|\widetilde{14_1^+}\rangle = \alpha_{14}|14_1^+(+,+)\rangle + \beta_{14}|14_2^+(-,-)\rangle, \quad (4)$$

$$|\widetilde{13_1^+}\rangle = \alpha_{13}|13_1^+(-,-)\rangle + \beta_{13}|13_2^+(+,+)\rangle. \quad (5)$$

Here $|\ \rangle$ represents an original eigenstate and $|\widetilde{\ }\rangle$ represents an admixed state; for example, by an octupole interaction. Here $\alpha^2 + \beta^2 = 1$ and $|\alpha| \gg |\beta|$ are assumed for real parameters α and β.

Using the admixed state $|\widetilde{14_1^+}\rangle$ to reproduce the experimental $B(E2;14_1^+ \to 12_1^+)$ value, $\beta_{14} = 0.013$ is required. Here it is assumed that the 12_1^+ state is not mixed: $|\widetilde{12_1^+}\rangle = |12_1^+\rangle$. Then the experimental $B(M1;14_1^+ \to 13_1^+) = 1.9 \times 10^{-5}\mu_N^2$ is exactly reproduced by adopting the value of $\beta_{13} = 0.084$. This indicates that any parity-changing interaction between neutrons and protons should be very weak even if it exists.

The study of nearly degenerate doublet bands in doubly-odd nuclei has been a subject of special interest in recent years. A vast amount of experimental information about such pairs of bands built on the $(\nu h_{11/2}^{-1} \otimes \pi h_{11/2})$ configuration has been accumulated for the region of mass 130 [16–24]. Doublet bands with the $(\nu h_{11/2}^{-1} \otimes \pi h_{11/2})$ configuration have been investigated theoretically in the framework of the PTSM [5–8,11–13,25–30]. In the model, the collective nucleon pairs are assumed to be the building blocks for even-even nuclei. Additional unpaired neutron and proton are added to the even-even nuclear states in the description of doubly-odd nuclei. The energy spectra for the doublet bands were well reproduced, along with the characteristic behavior of the electromagnetic transitions [7,8,12,13]. Through the analysis of the PTSM wave functions, it has been confirmed that the doublet bands turn out to be constructed by a weak coupling of various angular-momentum configurations of the unpaired neutron and the unpaired proton, i.e., the *chopsticks configurations* [8,12,13], with the quadrupole collective excitations of the even-even part of the nucleus. The chopsticks configurations and the even-even core produce characteristic $M1$ and $E2$ bands.

Concerning the $(\nu h_{11/2}^{-1} \otimes \pi h_{11/2})$ configuration in ^{136}La, a slight staggering pattern is seen in the $B(M1)$ values. Thus the nature of this $(\nu h_{11/2}^{-1} \otimes \pi h_{11/2})$ configuration has also been confirmed through the present study.

IV. SUMMARY

A large-scale shell model calculation has been performed for ^{136}La. Energy levels and transition rates have been calculated. The isomerism of the 14_1^+ state has been investigated. It has been found that the 14_1^+ state consists of the $(+,+)$ configuration; in contrast, the 9_1^+, 10_1^+, 11_1^+, 12_1^+, and 13_1^+ states are members of the group with the $(\nu h_{11/2}^{-1} \otimes \pi h_{11/2})$ configuration. This strongly indicates that the band crossing occurs at the 14_1^+ state. This structural change naturally explains why the 14_1^+ state becomes an isomer.

The yrast band structure with the $(\nu h_{11/2}^{-1} \otimes \pi h_{11/2})$ configuration has been also analyzed. Theoretical results show the staggering nature of the $M1$ transition rates, which indicates the nature of the chopsticks configuration for the states with the $(\nu h_{11/2}^{-1} \otimes \pi h_{11/2})$ configuration.

ACKNOWLEDGMENTS

This work was supported by Grants-in-Aid for Scientific Research (C) (No. 24540251 and No. 25400267) from Japan Society for the Promotion of Science (JSPS), and also by a Grant-in-Aid for JSPS Fellows, Grant No. 26.10429.

[1] E. W. Cybulska, J. R. B. Oliveira, M. A. Rizzutto, R. V. Ribas, N. H. Medina, W. A. Seale, M. N. Rao, F. R. Espinoza-Qui, J. A. Alcantara-Nunez, and F. Falla-Sotelo, Acta Phys. Pol. B **32**, 929 (2001).

[2] S. J. Zhu, S. D. Xiao, X. L. Che, Y. N. U, M. L. Li, Y. J. Chen, L. H. Zhu, G. S. Li, S. X. Wen, and X. Wu, Eur. Phys. J. A **24**, 199 (2005).

[3] T. Bhattacharjee, S. Chanda, S. Bhattacharyya, S. K. Basu, R. K. Bhowmikc, S. Muralithar, R. P. Singh, N. S. Pattabiramand, S. S. Ghugre, U. Datta, Pramanik, and S. Bhattacharya, Nucl. Phys. A **750**, 199 (2005).

[4] H. Nishibata, R. Leguillon, A. Odahara, T. Shimoda, C. M. Petrache, Y. Ito, J. Takatsu, K. Tajiri, N. Hamatani, R. Yokoyama, E. Ideguchi, H. Watanabe, Y. Wakabayashi, K. Yoshinaga, T. Suzuki, S. Nishimura, D. Beaumel, G. Lehaut, D. Guinet, P. Desesquelles, D. Curien, K. Higashiyama, and N. Yoshinaga, Phys. Rev. C **91**, 054305 (2015).

[5] K. Higashiyama, N. Yoshinaga, and K. Tanabe, Phys. Rev. C **67**, 044305 (2003).

[6] N. Yoshinaga and K. Higashiyama, Phys. Rev. C **69**, 054309 (2004).

[7] K. Higashiyama and N. Yoshinaga, Phys. Rev. C **83**, 034321 (2011).

[8] K. Higashiyama and N. Yoshinaga, Phys. Rev. C **88**, 034315 (2013).

[9] K. Higashiyama, N. Yoshinaga, and K. Tanabe, Phys. Rev. C **65**, 054317 (2002).

[10] E. Teruya, N. Yoshinaga, K. Higashiyama, and A. Odahara, Phys. Rev. C **92**, 034320 (2015).
[11] N. Yoshinaga and K. Higashiyama, J. Phys. G **31**, S1455 (2005).
[12] K. Higashiyama, N. Yoshinaga, and K. Tanabe, Phys. Rev. C **72**, 024315 (2005).
[13] K. Higashiyama and N. Yoshinaga, Prog. Theor. Phys. **113**, 1139 (2005).
[14] N. Yoshinaga and K. Higashiyama, Eur. Phys. J. A **30**, 343 (2006).
[15] T. Morek, H. Beuscher, B. Bochev, T. Kutsarova, R. Lieder, M. Muller-Veggian, and A. Neskakis, Nucl. Phys. A **433**, 159 (1985).
[16] K. Starosta, T. Koike, C. J. Chiara, D. B. Fossan, D. R. LaFosse, A. A. Hecht, C. W. Beausang, M. A. Caprio, J. R. Cooper, R. Krücken, J. R. Novak, N. V. Zamfir, K. E. Zyromski, D. J. Hartley, D. L. Balabanski, J.-y. Zhang, S. Frauendorf, and V. I. Dimitrov, Phys. Rev. Lett. **86**, 971 (2001).
[17] A. A. Hecht, C. W. Beausang, K. E. Zyromski, D. L. Balabanski, C. J. Barton, M. A. Caprio, R. F. Casten, J. R. Cooper, D. J. Hartley, R. Krücken, D. Meyer, H. Newman, J. R. Novak, E. S. Paul, N. Pietralla, A. Wolf, N. V. Zamfir, J.-Y. Zhang, and F. Dönau, Phys. Rev. C **63**, 051302 (2001).
[18] R. A. Bark, A. M. Baxter, A. P. Byrne, G. D. Dracoulis, T. Kibédi, T. R. McGoram, and S. M. Mullins, Nucl. Phys. A **691**, 577 (2001).
[19] K. Starosta, C. J. Chiara, D. B. Fossan, T. Koike, T. T. S. Kuo, D. R. LaFosse, S. G. Rohoziński, C. Droste, T. Morek, and J. Srebrny, Phys. Rev. C **65**, 044328 (2002).
[20] T. Koike, K. Starosta, C. J. Chiara, D. B. Fossan, and D. R. LaFosse, Phys. Rev. C **67**, 044319 (2003).
[21] G. Rainovski, E. S. Paul, H. J. Chantler, P. J. Nolan, D. G. Jenkins, R. Wadsworth, P. Raddon, A. Simons, D. B. Fossan, T. Koike, K. Starosta, C. Vaman, E. Farnea, A. Gadea, T. Kröll, R. Isocrate, G. deAngelis, D. Curien, and V. I. Dimitrov, Phys. Rev. C **68**, 024318 (2003).
[22] A. J. Simons, P. Joshi, D. G. Jenkins, P. M. Raddon, R. Wadsworth, D. B. Fossan, T. Koike, C. Vaman, K. Starosta, E. S. Paul, H. J. Chantler, A. O. Evans, P. Bednarczyk, and D. Curien, J. Phys. G **31**, 541 (2005).
[23] S. Wang, Y. Liu, T. Komatsubara, Y. Ma, and Y. Zhang, Phys. Rev. C **74**, 017302 (2006).
[24] I. Kuti, J. Timár, D. Sohler, E. S. Paul, K. Starosta, A. Astier, D. Bazzacco, P. Bednarczyk, A. J. Boston, N. Buforn, H. J. Chantler, C. J. Chiara, R. M. Clark, M. Cromaz, M. Descovich, Z. Dombrádi, P. Fallon, D. B. Fossan, C. Fox, A. Gizon, J. Gizon, A. A. Hecht, N. Kintz, T. Koike, I. Y. Lee, S. Lunardi, A. O. Macchiavelli, P. J. Nolan, B. M. Nyakó, C. M. Petrache, J. A. Sampson, H. C. Scraggs, T. G. Tornyi, R. Wadsworth, A. Walker, and L. Zolnai, Phys. Rev. C **87**, 044323 (2013).
[25] N. Yoshinaga, Nucl. Phys. A **503**, 65 (1989).
[26] N. Yoshinaga and D. M. Brink, Nucl. Phys. A **515**, 1 (1990).
[27] N. Yoshinaga, Nucl. Phys. A **570**, 421 (1994).
[28] N. Yoshinaga, T. Mizusaki, A. Arima, and Y. D. Devi, Prog. Theor. Phys. Suppl **125**, 65 (1996).
[29] N. Yoshinaga, Y. D. Devi, and A. Arima, Phys. Rev. C **62**, 024309 (2000).
[30] T. Takahashi, N. Yoshinaga, and K. Higashiyama, Phys. Rev. C **71**, 014305 (2005).